*Radiophysics and Quantum Electronics, Vol. 49, No. 10, 2006*

# NUMERICAL SIMULATION OF LOW-FREQUENCY OSCILLATIONS OF THE SPACE CHARGE AND POTENTIAL IN THE ELECTRON-OPTICAL SYSTEM OF A GYROTRON

**V. N. Manuilov** *

UDC 621.385.6

*We present the results of simulating magnetron-injection guns of gyrotrons using the PIC technique for large values of the pitch factor, in which case intense oscillations of the space charge cloud and the related oscillations of the potential in the beam are observed. Time dependences are found for the charge located in the adiabatic trap. The temporal evolution of the potential in different cross sections of the beam and the corresponding frequency spectra are calculated. The process of reflected-particle bombardment of the cathode and the role of the secondary electron emission in the process of particle accumulation in the trap are studied. The beam parameters for regimes with a great share of trapped particles are found and compared with those calculated within the framework of the static model. Time dependences of the current of the beam entering the operating space are analyzed and the electron energy distribution at the input of the gyrotron cavity is found.*

## 1. INTRODUCTION

The output power and efficiency of gyrotrons are significantly dependent on the achievable average value of the pitch factor $g$ (the ratio of the rotational and longitudinal velocities of the particles in the operating space) in the helical electron beam (HEB) acting as a source of radiation energy. For many reasons, magnetron-injection guns (MIGs) used in the overwhelming majority of gyrotrons [1] form HEBs with a significant (20–30% and more) spread of rotational velocities [2]. At the same time, the characteristic feature of a MIG is the mirror magnetic-field distribution [1], which, along with the above-mentioned value of the velocity spread, leads to reflection of a significant portion of particles from the magnetic mirror even at moderate values $g \approx 1.3$–$1.5$ of the pitch factor [3]. Then such electrons are reflected from the electron mirror in the vicinity of the MIG cathode and are trapped in the adiabatic trap between the cathode and the operating space of the device. The trapped particles are accumulated in the trap, which deteriorates the beam quality and frequently leads to instability of the beam [2]. The appearance of the instability is related to development of oscillations of the space charge and potential in the beam. Therefore, studies of these oscillations allow one to determine ways for improving the beam quality and predict its parameters with greater accuracy.

The first theoretical works dealing with oscillations of the potential in intense HEBs [4, 5] used a one-dimensional model of the adiabatic trap. A definite advantage of this model is the possibility to analyze long time intervals comprising hundreds of periods of longitudinal particle oscillations in the trap. However, the one-dimensional model does not take into account a number of factors that favor both accumulation and "leakage" of the space charge out of the trap, including such an important factor as secondary emission

* manuilov@rf.unn.ru

N. I. Lobachevsky State University of Nizhny Novgorod, Nizhny Novgorod, Russia. Translated from Izvestiya Vysshikh Uchebnykh Zavedenii, Radiofizika, Vol. 49, No. 10, pp. 872–879, October 2006. Original article submitted April 20, 2006; accepted November 2, 2006.

 

from the cathode [6]. In what follows we present the results of simulating the MIG on the basis of a more comprehensive model [6, 7] allowing for a two-dimensional distribution of the space charge in the HEB, the influence of thermal velocities, roughness of the emitter, and the secondary emission from the cathode. The time scales, amplitudes, and frequency spectra of oscillations of the potential, which are typical of the processes of transition of the electron cloud to the quasistationary state, are found. The beam parameters are compared with the data of the static model of the beam. Several feasible methods of reducing the oscillations are indicated.

## 2. BRIEF DESCRIPTION OF THE SIMULATION TECHNIQUE AND THE STUDIED MIG

Numerical simulation was performed using the PIC technique [7] with allowance for the secondary emission of electrons from the cathode [6] within the framework of the following assumptions:

(i) axial symmetry;

(ii) constant temperature of the cathode;

(iii) operation of the gun in the regime of temperature limitation of the emission;

(iv) presence of emitter roughness and the spread of initial electron velocities [2, 9].

To allow for the last two factors, we introduced a nearly Gaussian function of electron distribution over initial azimuthal velocities in accordance with [8]. The width of the function was chosen such that the calculated relative velocity spread $\delta v_\perp$ in the cold regime (when one can neglect the effect of the space-charge forces) was close to 20%. This value of $\delta v_\perp$ is typical for gyrotron MIGs [3, 10].

We considered the MIG of a centimeter-wavelength gyrotron operated in the weakly supercritical regime (see Fig. 1) and forming a beam with regular intersections of electron trajectories. In particular, such a beam is typical of the gyrotrons used in technological facilities for microwave material processing (synthesis of various ceramics, etc.). Choice of the MIG of such a type makes it possible to perform calculations within an acceptable time. In high-power gyrotrons for fusion experiments, the elevation of electron trajectories over the emitter and the scales of the trajectories (the pitch and radius of rotation) are significantly smaller [3], which sharply increases the calculation time. At the same time, it is evident that the main physical processes in both cases should be similar.

We studied the diode version of the gun with the accelerating voltage $U_0 = 60$ kV and geometry close to that of the gun of a high-power gyrotron operated at the second cyclotron harmonic [9] (operating wave-

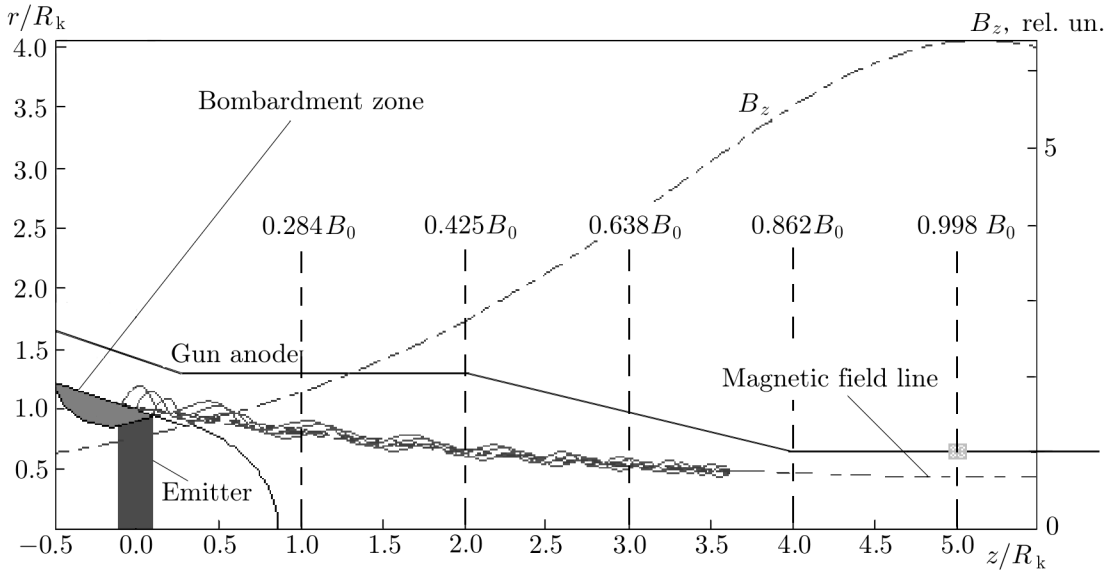


Fig. 1. Shape of MIG electrodes and the ratio of the current value $B_z(z)$ of the magnetic field to the operating field $B_0$ in different planes. The behavior of electron trajectories and the guiding magnetic-field line are shown. The longitudinal ($z$) and radial ($r$) coordinates are normalized to the average radius $R_k$ of the gun emitter.

length is about 12.5 mm). The regime of the gun was chosen such as to ensure the value of the "cold" pitch factor in the range $1.6 < g_0 < 2$. The corresponding value of $g_0$ was chosen by adjusting the magnetic-field distribution. The current $I_0$ of the gun was chosen equal to $0.1I_{\rm L}$, where $I_{\rm L}$ is the current calculated by Child's law for the cathode–anode gap of the gun in the emitter region ($I_{\rm L} \approx 275$ A). Secondary-emission constants of the cathode were taken the same as for molybdenum (the maximum secondary-emission coefficient was 1.25, and the electron energy corresponding to it, 375 eV). The calculations were performed up to the time instant $t = 40T_{\parallel}$, where $T_{\parallel}$ is the average time of electron transit from the cathode to the operating space.

## 3. OSCILLATIONS OF THE SPACE CHARGE AND POTENTIAL

Figure 2 illustrates the process of accumulation of the space charge in the trap for the large pitch factor $g_0 = 2$. Here, $Q_{\rm r}$ is the trapped charge, $Q_0$ is the charge of the initial beam (i.e., electrons flying towards the operating space and not reflected from the magnetic mirror yet). According to Fig. 2, after the end of transient processes, regular oscillations of the value of the trapped space charge begin in the beam. The amplitude of the oscillations reaches 5–10% of the average value of $Q_{\rm r}$. The period of the oscillations is close to the average period $2T_{\parallel}$ of longitudinal oscillations of the particles in the trap, and the onset time is about $(16\text{–}20)T_{\parallel}$. It is interesting that for $g_0 = 2$, the quantity $Q_{\rm r}$ is even greater than the charge $Q_0$ of the initial beam. Note that $Q_{\rm r}$ is strongly dependent on the pitch factor. For example, reducing $g_0$ from 2 to 1.6 causes a four-fold decrease in $Q_{\rm r}$. Correspondingly, for small $g_0$ (1.6 and smaller), the oscillations have quasi-noise character, and their amplitude decreases by more than an order of magnitude.

If secondary emission is not taken into account in numerical simulation, then the value of the trapped charge decreases by five times even for $g_0 = 2$ and only small quasi-noise oscillations are observed in the beam. Thus, secondary emission is one of the main factors which determine development of space-charge oscillations in the beam. Therefore, all the data presented in what follows were obtained with allowance for secondary emission.

It is evident that oscillations of the space charge also lead to oscillations of the potential in the beam (see Fig. 3). For small values of the pitch factor ($g_0 = 1.6$), the oscillations have quasi-noise character (see the lower curve in Fig. 3). However, their amplitude rapidly increases with increasing $g_0$, and for $g_0 = 2$, the

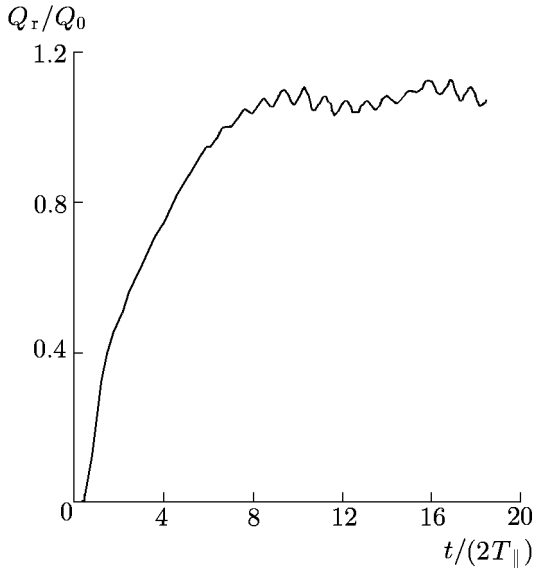


Fig. 2. Ratio of the trapped charge to the charge of the initial beam as a function of time for $g_0 = 2$.

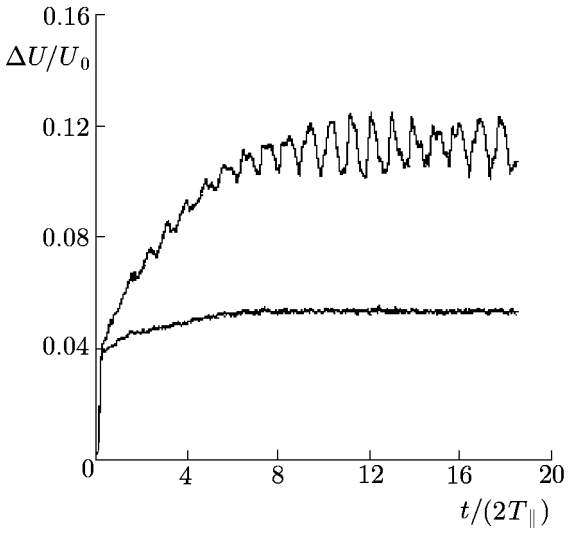


Fig. 3. Dependence of the potential sag $\Delta U$ on time in the plane $z/R_{\rm k} = 3.5$ with the most intense oscillations. The upper and lower curves were calculated for $g_0 = 2$ and $g_0 = 1.6$, respectively.

oscillations acquire a pronounced periodic character in all parts of the beam-forming system. The oscillation amplitude $U_{\rm amp}$ reaches its maximum value near the reflection plane $z/R_{\rm k} \approx 4$, where it exceeds 1% of the total accelerating potential of the beam (i.e., 600 V in the case under consideration). Then it decreases and becomes approximately four times lower in the operating space (Fig. 4).

After the end of the transient process, the shape of the temporal dependence of the potential $U(t)$ becomes close to that found within the one-dimensional model for the same ratio $Q_{\rm r}/Q_0$ (see Fig. 1 in [4], which corresponds to $Q_{\rm r}/Q_0 \approx 1$ and $g = 1.4$). Thus, the main factor which determines the shape and amplitude of oscillations of the potential in the beam is the ratio of the trapped charge and the initial-beam charge. The time of oscillation development in the beam obtained within the framework of the two-dimensional model is significantly shorter. The reasons for these discrepancies are apparently related to the differences between the mechanisms of accumulation and leakage of the particles from the trap, which were taken into account in different models.

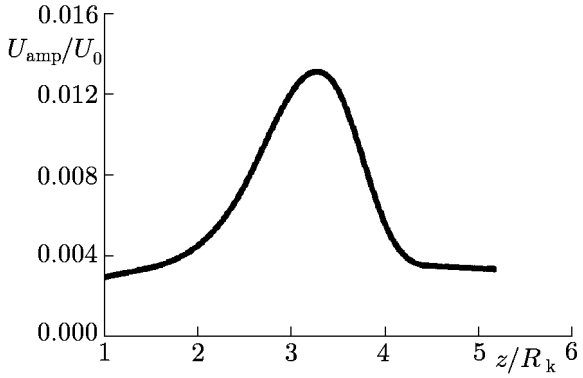


Fig. 4. Amplitude of oscillations of the potential as a function of the longitudinal coordinate for $g_0 = 2$.

Figure 5 shows the frequency spectra of the potential in different cross sections of the beam. It is evident that particles with different oscillatory velocities are reflected in different planes, which leads to a spread in the times of particle oscillations in the trap and to some widening of the corresponding frequency components in the spectrum. Probably, it is the presence of different, but close frequencies of longitudinal oscillations that leads to the appearance of the dependences $Q_{\rm r}(t)$ and $\Delta U(t)$ looking as beatings of oscillations with close frequencies (see Figs. 2 and 3). Elementary estimations show that for the character of the beatings shown in Figs. 1, 2, and 3, the difference of the corresponding frequencies must be about 20%. The presence of the beatings leads to the appearance of a low-frequency component in the spectrum with characteristic frequency $0.1/T_{\|}$.

The oscillation spectrum is abundant in the higher harmonics in the vicinity of the cathode (Fig. 5*a*). In the region of most intense oscillations (in front of the magnetic mirror), the first harmonic is predominant in the spectrum (Fig. 5*b*). In the operating space, the amplitude of oscillations decreases, and only the first and second harmonics are discernible in the spectrum (Fig. 5*c*).

Complication of the frequency spectra is apparently related to the transformation of the function of electron distribution over oscillatory velocities from the Gaussian function into a multi-hump one. This transformation was noted many times in theoretical calculations [8, 10], which were performed on the basis of the static model of the beam. As a rule, the presence of reflected electrons in the beam makes the distortion of the distribution function even stronger and results in complication of the frequency spectrum.

## 4. ELECTRON BUNCHING AND BOMBARDMENT OF THE CATHODE

Intense oscillations of the potential lead to the appearance of a resonant time-periodic force from the side of the electric field, which affects the beam particles, supplies additional energy to a part of the particles, and causes longitudinal bunching of the reflected electrons. It is evident that at resonance (i.e., when the frequencies of electron oscillations in the trap and of the alternating component of the Coulomb field in the beam are close), the above-mentioned energy can be several times greater than the value $eU_{\rm amp}$ corresponding to the maximum amplitude $U_{\rm amp}$ of oscillations of the potential (here, $e$ is the electron charge). This energy is sufficient for the reflected electrons to overcome the potential barrier near the cathode and bombard its surface. Calculations show that the average energy of electrons bombarding the cathode is close to 3% of that corresponding to the accelerating potential, i.e., it exceeds $eU_{\rm amp}$ by approximately three times. This value of the energy of the electrons bombarding the cathode is close to that measured in [5]. The

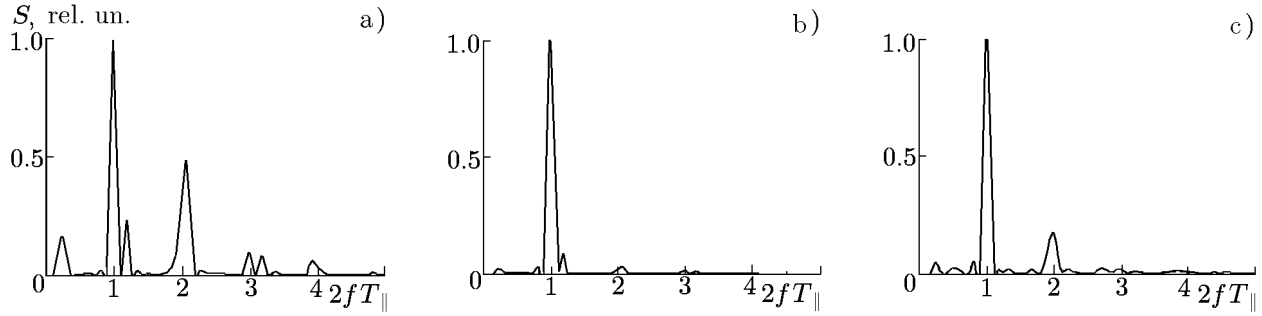


Fig. 5. Normalized frequency spectra $S(f)$ of oscillations of the potential, calculated for $g_0 = 2$ and different planes: $z/R_\mathrm{k} = 1.0$ (*a*), $z/R_\mathrm{k} = 3.5$ (*b*), and $z/R_\mathrm{k} = 5.2$ (*c*).

bombardment zone is approximately three times wider than the emitter and is shifted to the region with a weaker magnetic field (see Fig. 1).

Electron bunches coming to the cathode region cause periodic bombardment of the cathode. As a result, both the average energy of the electrons bombarding the cathode and the position of the left-hand boundary of the bombardment area oscillate in time (Figs. 6 and 7). It is interesting that the position of the right-hand boundary of the bombardment region varies only slightly in time. The majority of the particles cross the cathode from the left of the emitter boundaries (Fig. 8).

## 5. PARAMETERS OF THE ELECTRON BEAM IN THE OPERATING SPACE OF A GYROTRON

Accumulation of the reflected particles in the adiabatic trap changes beam parameters. Table 1 shows the values of the pitch factor calculated on the basis of the static and dynamic models for the regimes with the operating current $I_0 = 0.1 I_\mathrm{L}$. It is seen that the dynamic model yields much lower values of $g$ due to the additional screening of the electric field at the emitter by the trapped charge.

According to the calculation data, the current entering the operating space has an alternating component $I_\mathrm{var}(t)$ (see Fig. 9). The period of the dependence $I_\mathrm{var}(t)$ is close to the period of longitudinal oscillations of the particles in the trap, and the amplitude is about 5% of the average value of the current $I_0$. It should be noted that the value of $I_0$ depends on the secondary-emission coefficient of the cathode and can differ significantly from that calculated by the Richardson–Dushman equation.

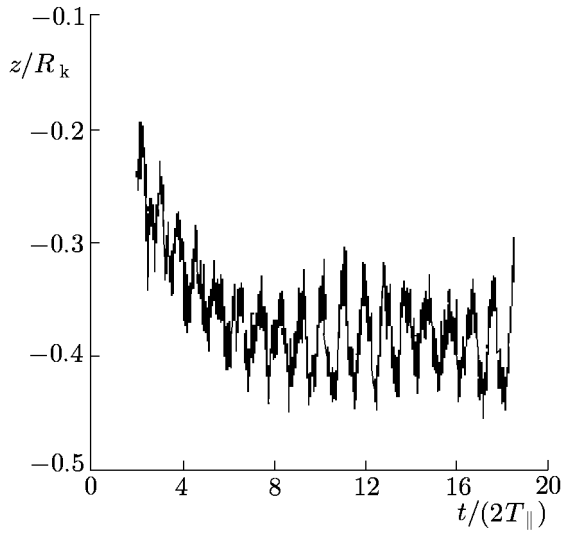


Fig. 6. Position of the left-hand boundary of the bombardment zone at various times for $g_0 = 2$.

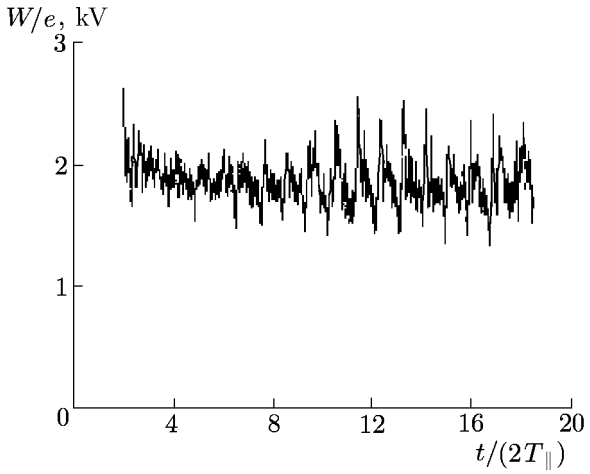


Fig. 7. Average energy $W$ of the electrons bombarding the cathode as a function of time for $g_0 = 2$.

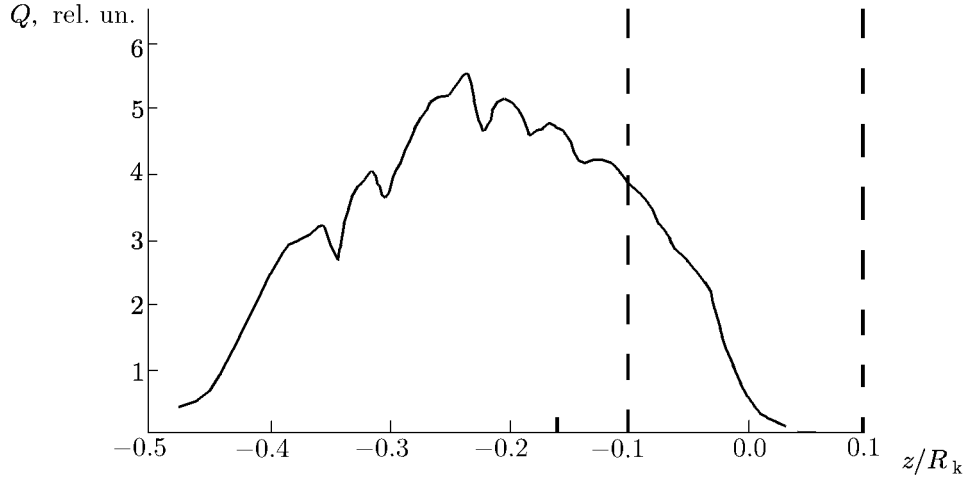


Fig. 8. Distribution of the charge of the particles bombarding the cathode along its surface. Dashed lines correspond to the emitter boundaries.

Oscillations of the potential also lead to a change in the energy distribution of the electrons coming to the operating space (see Fig. 10). It becomes wider compared with that in the static model (the width $\Delta W/e \approx$ (2–3) kV$\approx$ (0.03–0.05)$\,U_0$, whereas the potential sag across the beam is only $0.005U_0$) and shifts to the region of lower energies. As a result, the peak energy $W_\mathrm{p}$ of the electrons in the beam turns out to be lower than that corresponding to the potential $U_\mathrm{beam}$ of the beam (within the framework of the static model, evidently, $W_\mathrm{p} \approx eU_\mathrm{beam}$). This value of $\Delta W$ is in satisfactory agreement with the results of measuring the energy spectrum of the electrons in high-power gyrotrons for moderate pitch factors [10]. Note that the share of the accelerated electrons with the energy $W > eU_\mathrm{beam}$ increases from 5% for $g_0 = 1.6$ up to 15–17% in the case where $g_0$ reaches 2. The average energy of the electrons coming to the operating space oscillates in time with a frequency close to the frequency of longitudinal oscillations of the particles in the adiabatic trap.

## 6. CONCLUSIONS

The results of numerical simulation show that for large values of the "cold" pitch factor (close to 2), the charge located in the adiabatic trap becomes comparable with the charge of the initial beam. Under such conditions, intense oscillations of the space charge and potential develop in the beam-formation region. The amplitude of oscillations of the potential can reach approximately 1% of the accelerating potential. These oscillations cause longitudinal bunching of the trapped particles and their additional acceleration. A part of the accelerated particles bombard the cathode and cause secondary emission from the cathode. The current and energy of the electrons bombarding the cathode, as well as the position of the left-hand boundary of the bombardment region oscillate in time with the frequency of the longitudinal oscillations of the particles in the trap. Secondary emission is the main source of the particles trapped in the beam. The space charge of the trapped particles leads to a significant decrease in the value of the pitch factor in the beam.

For large values of the pitch factor, the beam entering the operating space turns out to be premodulated with respect to the current and energy of the particles at the frequency of longitudinal oscillations. The width of the energy distribution in the beam is 2–4% of the accelerating potential, and the alternating component of the current can reach 1–5% of the average value.

TABLE 1. Values of the pitch factor $g$ calculated on the basis of different models.

| "Cold" pitch factor $g_0$ | Static model | Dynamic model |
|---|---|---|
| 1.6 | 1.45 | 1.38 |
| 2.0 | 1.73 | 1.45 |

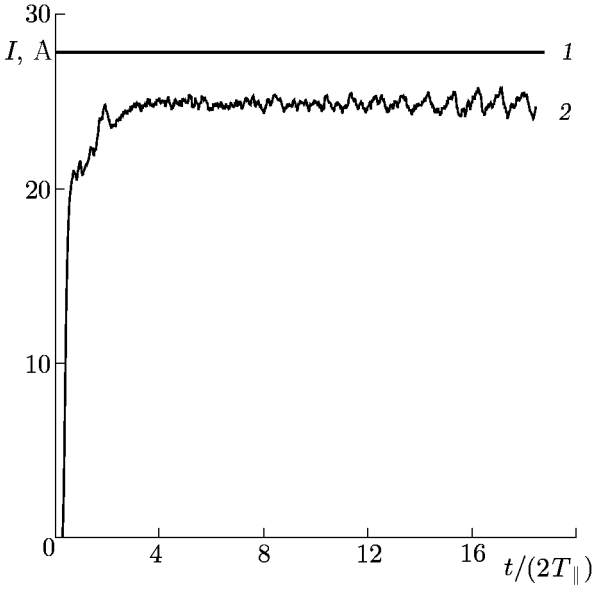


Fig. 9. Time dependence of the current entering the operating space for $g_0 = 2$: curve *1* corresponds to the static model, while curve *2*, to the dynamic model.

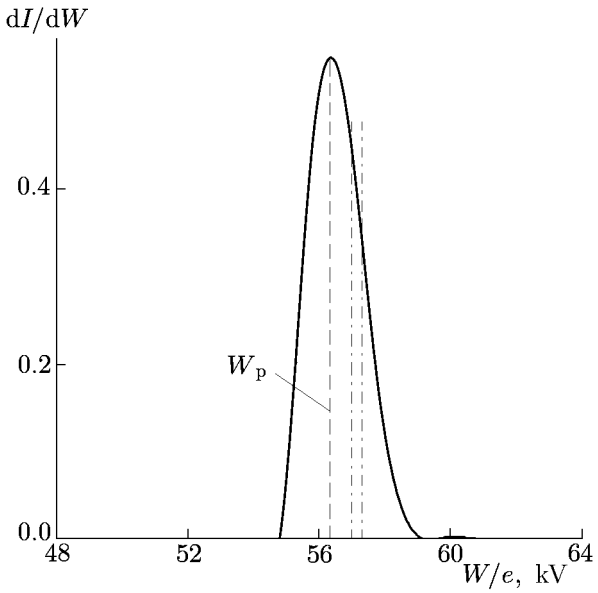


Fig. 10. Energy distribution of the electrons entering the operating space ($z/R_k = 5.15$) for $g_0 = 2$. Dash-dot lines correspond to the maximum and minimum values of the potential during its oscillations.

To lower the intensity of the oscillations, it is necessary to reduce the share of the space charge located in the adiabatic trap, primarily by reducing the secondary emission from the cathode.

The author is grateful to V. L. Bratman, M. Yu. Glyavin, V. E. Zapevalov, and A. N. Kuftin for useful discussions of the described results and to V. Yu. Zaslavsky for help with the processing of the calculation results.

This work was supported by the Russian Foundation for Basic Research (project Nos. 05–02–16015 and 05–02–08024-ofi-a) and the INTAS (project No. 03–51–3861).

**REFERENCES**

1. A. L. Gol'denberg and M. I. Petelin, *Radiophys. Quantum Electron.*, **16**, No. 1, 106 (1973).
2. Sh. E. Tsimring, *Int. J. Infrared Millimeter Waves*, **22**, 1433 (2001).
3. A. N. Kuftin, V. K. Lygin, Sh. E. Tsimring, and V. E. Zapevalov, *Int. J. Electron.*, **72**, Nos. 5–6, 1145 (1992).
4. D. V. Borzenkov and O. I. Louksha, *Tech. Phys.*, **42**, No. 9, 1071 (1997).
5. O. I. Louksha, G. G. Sominski, and D. V. Kas'yanenko, in: *Proc. Int. University Conf. "Electronics and Radiophysics of Ultra-High Frequencies," St. Petersburg, Russia, May 24–28, 1999*, p. 130.
6. P. V. Krivosheev and V. N. Manuilov, *Prikl. Fiz.*, No. 3, 80 (2002).
7. P. V. Krivosheev, V. K. Lygin, V. N. Manuilov, and Sh. E. Tsimring, *Int. J. Infrared Millimeter Waves*, **22**, No. 8, 1119 (2001).
8. V. K. Lygin, *Int. J. Infrared Millimeter Waves*, **16**, No. 2, 363 (1995).
9. Sh. E. Tsimring, *Radiophys. Quantum Electron.*, **15**, No. 8, 952 (1972).
10. A. N. Kuftin, V. K. Lygin, V. N. Manuilov, et al. *Int. J. Infrared Millimeter Waves*, **20**, No. 3, 361 (1999).